ACS Catalysis

Research Article

pubs.acs.org/acscatalysis

Tailoring the Oxidation Activity of Pt Nanoclusters via Encapsulation

Fan Zhang,[†] Feng Jiao,[†] Xiulian Pan,*[,†] Kang Gao,[‡] Jianping Xiao,[†] Shuo Zhang,[∥] and Xinhe Bao*[,†]

[†]State Key Laboratory of Catalysis, Dalian Institute of Chemical Physics, Chinese Academy of Sciences, Dalian 116023, China

[‡]School of Chemical Engineering, Dalian University of Technology, Dalian 116023, China

[∥]Shanghai Synchrotron Radiation Facility, Shanghai Institute of Applied Physics, Chinese Academy of Sciences, Shanghai 201204, China

S *Supporting Information*

ABSTRACT: To tailor the catalytic activities of metal catalysts at will to achieve efficient conversion in chemical processes remains a challenge, particularly for noble metals, such as Pt. We demonstrate herein that encapsulation within the carbon nanotube (CNT) channels with a diameter of 1.0−1.5 nm not only allows restriction of the size of Pt nanoclusters around 1.0 nm but also enables modulating of the Pt species at the active reduced states through host−guest interaction. The encapsulated Pt is protected from oxygen under reaction conditions in toluene oxidation up to 200 °C, as unveiled by in situ X-ray absorption spectroscopy and density functional theory calculations. As a result, the encapsulated Pt clusters deliver a remarkably higher activity and stability than the clusters located on the open surfaces of the CNT exterior walls and carbon black support, although the latter are much more accessible to reactants. This characteristic of the CNT channels can be explored to tune the properties of other metal catalysts for oxidation reactions.

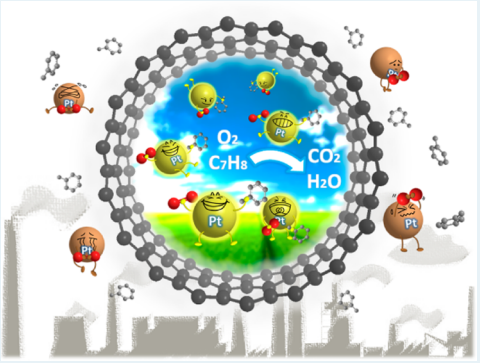

KEYWORDS: *platinum, cluster, confined catalysis, carbon nanotube, toluene oxidation*

INTRODUCTION

Pt is a versatile noble metal catalyst for a wide range of industrial processes, including catalytic oxidation of volatile organic compounds (VOCs) in industrial gaseous pollutants.[1,2] The high price and scarce reserves of noble metals have impelled wide efforts to improve the utilization efficiency. In particular, it has been demonstrated that reducing the size of metal nanoparticles down to a few nanometers, and even subnanometer scale, is an efficient approach because they exhibit significantly higher activities than larger nanoparticles.[3−9] For instance, it was reported that Pt clusters with a size around 1.0 nm supported on interconnected porous $CaMnO_3$ nanoparticles give a much higher mass and specific activity in oxygen reduction reaction relative to commercial carbon-supported Pt nanoparticles with a larger size.[3] Subnanometer Pt clusters distributed on a graphene nanosheet showed an unusually high activity for methanol oxidation compared with conventional Pt nanoparticles (2−3 nm) supported on carbon black.[6] However, these fine nanoclusters are unsaturatedly coordinated and prone to aggregation, especially under reaction conditions. Therefore, surfactants, polymers, and dendrimers are frequently indispensable to stabilize them and to control their size.

Hossain et al. synthesized Pt nanoparticles with an average diameter of 1.4 ± 0.3 nm using poly(*N*-vinyl-2-pyrrolidone) as a stabilizer.[10] Yamamoto et al. developed a method to prepare Pt subnanometer-sized nanoclusters, Pt_{12}, with a fourth-generation pheylazomethine dendrimer loaded onto a mesoporous carbon support, which exhibited a high activity in oxygen reduction[8] and hydrogenation of low-reactive olefins.[11] Li et al. and Witham et al. used hydroxyl-terminated polyamidoamine dendrimers to encapsulate Pt_{40} clusters on a silica support, SBA-15.[12,13] The resulting catalysts gave a high selectivity and exceptional recyclability for multiple uses in a series of solution-phase electrophilic π-bond activation reactions.[12,13] However, the choice of surfactants and dendrimers is reaction-specific, which may have steric effects shielding the active sites from access by certain reactants and may also modify the electronic environment of the metal centers and, hence, their catalytic activity.[14] On the other hand, the relatively poor thermal stability of the organic capping agent could hinder their utilization in higher temperature reactions.

Furthermore, fine metal clusters are prone to oxidation in an oxygen atmosphere, particularly at higher temperatures, which frequently leads to deactivation. An elegant approach reported recently is to confine metal centers within the lattice of the support materials, which can stabilize the under-coordinated metal sites and even isolated atoms.[15] Alternatively, support materials with well-defined pore structures, such as zeolite,[16] metal organic frameworks,[17] and carbon nanotubes (CNTs),[18−20] have also been used to encapsulate metal clusters. For example, a CNT can be considered as a graphene

Received: November 7, 2014
Revised: December 19, 2014
Published: January 28, 2015

DOI: 10.1021/cs501763k
ACS Catal. 2015, 5, 1381−1385

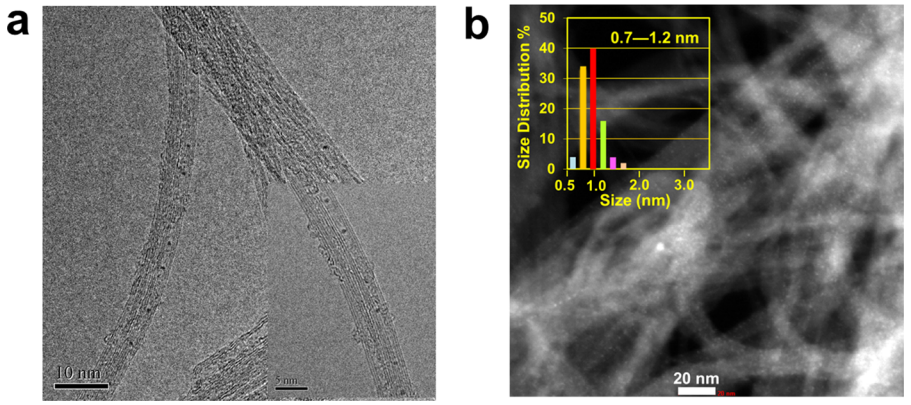

Figure 1. (a) HRTEM image with the inset showing discrete clusters encapsulated within the CNT channels; (b) HAADF-STEM image with the size distribution of Pt clusters in the inset showing that most particles fall in a range of 0.7−1.2 nm.

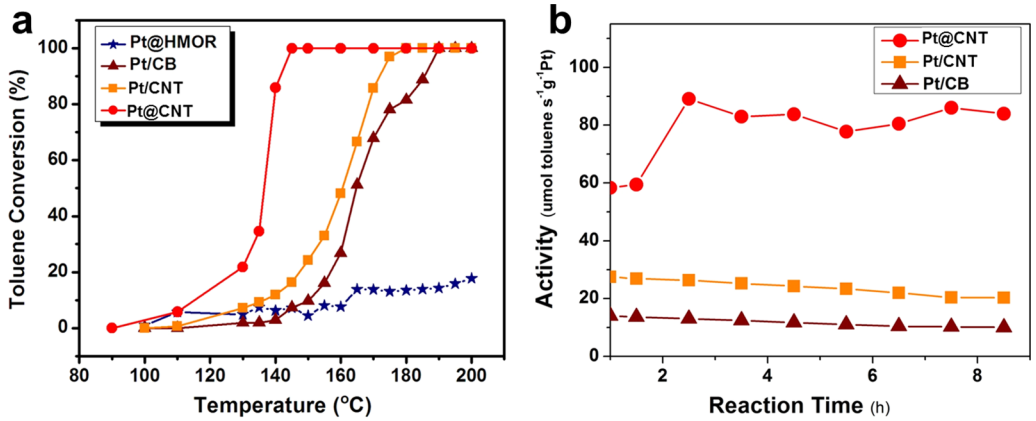

Figure 2. Activities and stability of Pt@CNT in comparison with Pt clusters exposed on open surfaces of the CNT exterior walls and CB (Pt/CNT and Pt/CB): (a) toluene conversion as a function of reaction temperatures; (b) the stability test.

layer rolling up to form the tubular morphology, where a variety of nanostructured materials have been entrapped.[21,22] The confined metal nanoparticles showed intriguing catalytic activity in various reactions, for example, Fischer−Tropsch synthesis,[23] asymmetric hydrogenation,[24] and hydrogenation reactions in the supercritical CO_2 phase.[25] More interestingly, within the confined environment of CNTs, oxidation of metallic iron was hindered compared with those located on the exterior walls.[26] We wonder if CNTs will exert a similar protection effect on the extremely active Pt nanoclusters. Therefore, we introduced Pt nanoclusters with a size around 1 nm within the CNT channels with an inner diameter of 1.0−1.5 nm, and investigated their catalytic activity and stability, taking the oxidation of toluene as a model. This is an important industrial process to remove VOC and has been widely studied as a prototype reaction. The encapsulated Pt clusters deliver a much higher activity with a stable performance than the clusters distributed on the open surfaces of carbon black and the CNT exterior walls. In situ X-ray absorption near edge spectroscopy (XANES) reveals that encapsulation allows tailoring of the Pt clusters at the active metallic states throughout the reaction, in contrast to those easily oxidized on the open surface, which is confirmed by density functional theory (DFT) calculations.

RESULTS AND DISCUSSION

Highly purified thin-walled CNTs with an inner diameter of 1.0−1.5 nm were purchased from TimesNano Inc., which were produced by catalytic decomposition of methane. The ends of the CNTs were opened during purification and cut into sections shorter than 1 μm. Volatile (trimethyl)-cyclopentadienyl platinum was used as the precursor, following a procedure similar to that of our previous study.[27] The Pt complex on the exterior walls of CNTs was removed by excess ethanol. The sample was reduced in situ in H_2 prior to reaction (denoted as Pt@CNT) (see Supporting Information for more details). The HRTEM image in Figure 1a shows that discrete nanoclusters are distributed within the channels. The high-angle annular dark-field scanning transmission electron microscopy (HAADF-STEM) image of Figure 1b reveals that these nanoclusters are homogeneously distributed. Statistical analysis shows that more than 80% of the clusters fall in a size range of 0.7−1.2 nm. Because of the spatial restriction of the CNT channels, particles larger than 2 nm were scarcely observed. Further CO chemisorption shows that the average size of the encapsulated Pt nanoclusters is 1.3 nm. The dispersity of Pt reaches as high as 87%.

The reaction was carried out under atmospheric pressure in a quartz fixed-bed reactor in a temperature- programmed mode, from room temperature to 200 °C. An Ar flow containing 1000 ppm toluene and 20% oxygen was fed into the reactor. The effluents were analyzed by an online GC when the temperature had stabilized for at least 30 min. Complete oxidation to CO_2 is confirmed by an online GC equipped with TCD and FID (Figure S1) and a time-of-flight mass spectrometer. Figure 2a shows that the toluene starts to be converted by the confined Pt clusters at 110 °C. The conversion shoots up with an increase

DOI: 10.1021/cs501763k
ACS Catal. 2015, 5, 1381−1385

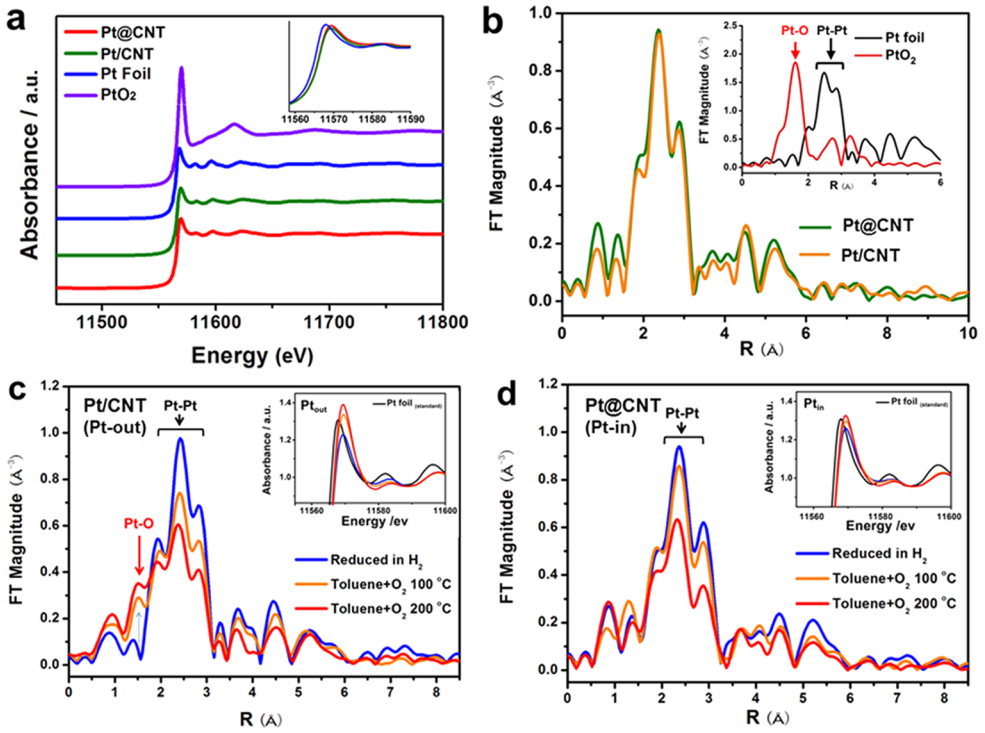

Figure 3. In situ XAFS of Pt catalysts during toluene oxidation. (a) The Pt L_{III} edge XANES spectra of reduced Pt@CNT with respect to those of Pt/CNT, Pt foil, and PtO_2 references. The inset shows the whiteline intensity of Pt@CNT is similar to that of Pt/CNT and Pt foil. (b) k^2-weighted EXAFS spectra with the inset showing those of reference samples Pt foil and PtO_2, which show their characteristic Pt−Pt and Pt−O bonds, respectively. (c) k^2-weighted EXAFS spectra of Pt/CNT during toluene oxidation at 100 and 200 °C with the inset showing the whiteline of the Pt L_{III} edge spectra along with the reduced Pt/CNT. (d) k^2-weighted EXAFS spectra of Pt@CNT during reaction under the same conditions as c, with the inset showing the whiteline of the Pt L_{III} edge spectra.

in the temperature to 130 °C, and it reaches 100% at 145 °C. In contrast, Pt nanoparticles dispersed on a commercially available, well graphitized carbon black (designed as Pt/CB) with 70% Pt clusters falling in a size range of 1.0−2.5 nm gives a lower activity (Figure S2), as toluene starts to be converted only above 120 °C. It does not reach a complete conversion until 185 °C, which is similar to other reported Pt catalysts.[28−31] Pt clusters with an average size of 1.0−2.0 nm were also distributed on the exterior walls of the same batch of CNTs as that of Pt@CNT (Figure S3) using the same precursor for comparison, denoted as Pt/CNT. This catalyst is obviously less active than Pt@CNT, similar to Pt/CB. The higher activity of Pt@CNT than Pt clusters exposed on the open surfaces of the exterior walls of CNTs and CB indicates the importance of encapsulation. However, further comparison with the zeolite H-mordernite HMOR reveals that it is more than just spatial restriction. Note that the loadings of the Pt of these four catalysts are close, in a range of 1.96−2.14% (weight percentage), as examined by inductively coupled plasma−atomic emission spectrometer (ICP−AES), as listed in Supporting Information Table S1.

Pt clusters were introduced into the pores of HMOR zeolite (with a pore size of 0.70 nm) in the parallel channel of the same reactor for Pt@CNT following the same procedure and conditions. The resulting catalyst, denoted as Pt@HMOR, exhibits very small clusters. The size of the discernible particles falls in a range of 0.4−0.7 nm (Figure S4). Figure 2a shows that this catalyst initiates toluene conversion around 110 °C, similar to Pt@CNT; however, toluene conversion is only 20%, even at the relatively high temperature of 200 °C, exhibiting a far lower activity than that over Pt@CNT. Obviously, solely spatial restriction and small particle size are not the key for the high activity observed for Pt@CNT.

For better comparison, the temperatures at which toluene conversion reaches 30% (T_{30}), and 100% (T_{100}) are listed in Table S2. The conversion rate in terms of converted toluene per second per gram of platinum ($\mu mol \cdot s^{-1} \cdot g^{-1}$ Pt) is also displayed. One sees that the activity of Pt@CNT is remarkably higher than other experimentally reported Pt catalysts, including Pt/Al_2O_3 with an averaged Pt particle size of 1.0 nm.[32] It was reported that the turnover frequency of Pt was found to decrease with a smaller particle size in oxidation of VOCs[32,33] as a result of the tendency of smaller Pt clusters to be oxidized in the presence of oxygen, as evidenced by a higher heat of oxygen chemisorption than that on larger Pt clusters.[33−35] Therefore, the confined environment of the CNT channels likely has modulated the states of the encapsulated Pt clusters.

This is confirmed by in situ XAFS, which allows monitoring of the structure evolution of Pt clusters under reaction conditions.[36−38] One sees that the XANES of the Pt L_{III} edge of the reduced Pt@CNT and Pt/CNT catalyst exhibit a feature similar to those of Pt foil (Figure 3a). Further comparison of the radial structural function (RSF) curves obtained from Fourier transformation of the EXAFS function, $\lambda(k)$, of momentum space (Figure 3b) also suggests the contribution of Pt−Pt interaction and the absence of Pt−O interaction. This confirms that Pt clusters in both Pt@CNT and Pt/CNT have been reduced fully prior to reaction and do not exhibit obvious differences.

The in situ RSF and Pt L_{III} edge of Pt/CNT (Figure 3c) show that the Pt−O scattering paths appear during oxidation of

DOI: 10.1021/cs501763k
ACS Catal. 2015, 5, 1381−1385

toluene and become more prominent with the increasing temperature. Meanwhile, the whiteline also becomes more intense (inset of Figure 3c). For noble metals such as Pt, the L_{III} edge XAS is derived from the electronic transition from $2p_{3/2}$ to 5d states. The whiteline intensity directly reflects the unoccupancy of 5d states and, thus, is a good indicator for oxidation state variation, as shown in previous studies.[12,39,40] This indicates that Pt species over the CNT exterior walls are oxidized during reaction. In contrast, the Pt−O scattering is hardly observable for Pt@CNTs (Figure 3d) under reaction conditions even up to 200 °C (in the presence of oxygen) with no significant change of the whiteline intensity (inset of Figure 3d). Furthermore, a lower coordination number, 0.5(7), and longer Pt−O bond, 2.13 ± 0.02 Å, are found for the encapsulated Pt clusters with respect to the coordination number of 1.2(5) and Pt−O bonds of 2.06 ± 0.02 Å for the outside Pt clusters from the first shell EXAFS analysis (Figure S5 and Table S3). Although it is difficult to discriminate between Pt−O and Pt−C observed for Pt/CNT at this stage, the results clearly demonstrate that encapsulation protects the fine Pt clusters, hindering its poisoning by either oxygen or other organic species under reaction conditions. Therefore, the confined catalyst is able to deliver a higher activity and stability in the oxidation of toluene, which requires reduced Pt as the active species. In contrast, the partially oxidized Pt species either because of oxygen or organic species on open surfaces, such as CB, and the CNT exterior walls are much less active, although they are much more accessible to reactants.

The capability of the CNT channels to protect the reduced metal species in the presence of oxygen is further validated by DFT calculations (see Supporting Information for details). CNT (18, 0) with a diameter of ∼1.5 nm and Pt_{43} clusters with a size of 0.96 nm encapsulated inside the channel were taken as models (Figure S6). We compared the oxidation reaction energy of Pt_{43} clusters inside and outside of the CNT channels because this reflects the affinity to oxygen, that is, the tendency to oxidation. A variety of adsorption sites and coverage of oxygen atoms were considered. Figure 4 shows that the

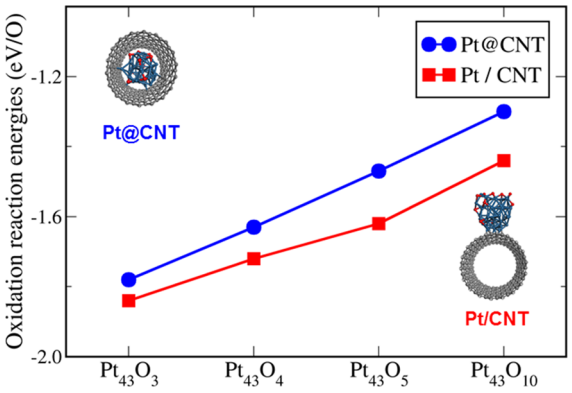

Figure 4. Averaged oxidation reaction energies per oxygen for Pt@CNT in comparison with Pt/CNT as a function of different oxygen coverages.

averaged oxidation reaction energy is about −1.72 eV/O, with four oxygen atoms on Pt/CNT. It decreases to −1.63 eV/O within the confined space of CNTs. The oxidation reaction energy further drops to −1.30 eV/O for Pt@CNT at the higher coverage with 10 oxygen atoms, corresponding to a higher extent of oxidation. This indicates that it is more difficult to oxidize the encapsulated Pt clusters than those on the open surface, which is consistent with in situ EXAFS.

The stability test over a longer period of time under reaction conditions further confirms the beneficial effects of confinement. A more severe testing condition that is, 2-fold weight hour space velocity (WHSV) was employed for Pt@CNT compared with Pt/CB and Pt/CNT. Figure 2b shows that the activity of Pt@CNT increases in the first 2 h and levels off in the following 7 h. In contrast, the activities of both Pt/CB and Pt/CNT decrease steadily and drop by 30% within 9 h. HRTEM image (Figure S7) shows that Pt clusters of Pt@CNT after reaction are limited to the range of 0.8−2 nm inside the channels. In comparison, without the spatial restriction, the particles of Pt/CNT grow larger, to 2−6 nm. Furthermore, Pt@HMOR loses activity even more quickly, and the used catalyst turns from the yellow of the fresh catalyst to dark brown. This is likely attributed to coke formation, similar to the previously reported Pt/HFAU[41] and Pt/HBEA,[42] leading to deactivation with time on stream. In this respect, CNTs have additional advantages of being devoid of strong acidic sites, consequently avoiding coke deposition and pore blocking during reaction. This demonstrates that encapsulation within CNTs enables limiting the aggregation of Pt nanoclusters and tailoring the Pt species at the active reduced states, even in the presence of oxygen up to 200 °C. Consequently, the encapsulated Pt delivers a much higher activity and more stable performance.

In summary, encapsulation within the CNT channels allows one to tailor the oxidation activity of Pt nanoclusters, not only by restricting the cluster size down to around 1.0 nm but, more importantly, by retaining the Pt species at the active reduced state, even in the presence of oxygen up to 200 °C. In contrast, clusters of a similar size dispersed on more open surfaces, such as commercial carbon black and the CNT exterior walls, are partially oxidized under the same conditions, leading to a significantly lower activity and stability in toluene oxidation, although the latter are much more accessible to reactants. The capability of the CNT channels' stabilizing reduced state metal clusters is expected to be a general feature, which can be explored to tailor the properties of other nanocatalysts for oxidation.

■ ASSOCIATED CONTENT

Supporting Information

The following file is available free of charge on the ACS Publications website at DOI: 10.1021/cs501763k

Experimental and calculation details; TEM and HAADF-STEM images of Pt/CB, Pt/CNT, and Pt@HMOR; TEM and HAADF-STEM images of Pt@CNT and Pt/CNT after the reaction; Tables S1−S3 (PDF)

■ AUTHOR INFORMATION

Corresponding Authors

*E-mail: panxl@dicp.ac.cn.

*E-mail: xhbao@dicp.ac.cn.

Notes

The authors declare no competing financial interest.

■ ACKNOWLEDGMENTS

P.X. and B.X. gratefully acknowledge Prof Y. Hu for kind help on discussions on XAFS results. This work was financially supported by the Natural Science Foundation of China (Grant

DOI: 10.1021/cs501763k
ACS Catal. 2015, 5, 1381−1385

nos: 11079005, 21033009, and 21173215) and the Ministry of Science and Technology (Grant no. 2011CBA00503 and 2013CB933100).

REFERENCES

(1) Armor, J. N. *Appl. Catal., B* **1992**, *1*, 221−256.
(2) Spivey, J. J. *Ind. Eng. Chem. Res.* **1987**, *26*, 2165−2180.
(3) Han, X. P.; Cheng, F. Y.; Zhang, T. R.; Yang, J. G.; Hu, Y. X.; Chen, J. *Adv. Mater.* **2014**, *26*, 2047−2051.
(4) Proch, S.; Wirth, M.; White, H. S.; Anderson, S. L. *J. Am. Chem. Soc.* **2013**, *135*, 3073−3086.
(5) King, J. S.; Wittstock, A.; Biener, J.; Kucheyev, S. O.; Wang, Y. M.; Baumann, T. F.; Giri, S. K.; Hamza, A. V.; Baeumer, M.; Bent, S. F. *Nano Lett.* **2008**, *8*, 2405−2409.
(6) Yoo, E.; Okata, T.; Akita, T.; Kohyama, M.; Nakamura, J.; Honma, I. *Nano Lett.* **2009**, *9*, 2255−2259.
(7) Qiao, B. T.; Wang, A. Q.; Yang, X. F.; Allard, L. F.; Jiang, Z.; Cui, Y. T.; Liu, J. Y.; Li, J.; Zhang, T. *Nat. Chem.* **2011**, *3*, 634−641.
(8) Yamamoto, K.; Imaoka, T.; Chun, W. J.; Enoki, O.; Katoh, H.; Takenaga, M.; Sonoi, A. *Nat. Chem.* **2009**, *1*, 397−402.
(9) Vajda, S.; Pellin, M. J.; Greeley, J. P.; Marshall, C. L.; Curtiss, L. A.; Ballentine, G. A.; Elam, J. W.; Catillon-Mucherie, S.; Redfern, P. C.; Mehmood, F.; Zapol, P. *Nat. Mater.* **2009**, *8*, 213−216.
(10) Hossain, M. J.; Tsunoyama, H.; Yamauchi, M.; Ichikuni, N.; Tsukuda, T. *Catal. Today* **2012**, *183*, 101−107.
(11) Takahashi, M.; Imaoka, T.; Hongo, Y.; Yamamoto, K. *Angew. Chem., Int. Ed.* **2013**, *52*, 7419−7421.
(12) Li, Y. M.; Liu, J. H. C.; Witham, C. A.; Huang, W. Y.; Marcus, M. A.; Fakra, S. C.; Alayoglu, P.; Zhu, Z. W.; Thompson, C. M.; Arjun, A.; Lee, K.; Gross, E.; Toste, F. D.; Somorjai, G. A. *J. Am. Chem. Soc.* **2011**, *133*, 13527−13533.
(13) Witham, C. A.; Huang, W. Y.; Tsung, C. K.; Kuhn, J. N.; Somorjai, G. A.; Toste, F. D. *Nat. Chem.* **2010**, *2*, 36−41.
(14) Chinthaginjala, J. K.; Villa, A.; Su, D. S.; Mojet, B. L.; Lefferts, L. *Catal. Today* **2012**, *183*, 119−123.
(15) Guo, X. G.; Fang, G. Z.; Li, G.; Ma, H.; Fan, H. J.; Yu, L.; Ma, C.; Wu, X.; Deng, D. H.; Wei, M. M.; Tan, D. L.; Si, R.; Zhang, S.; Li, J. Q.; Sun, L. T.; Tang, Z. C.; Pan, X. L.; Bao, X. H. *Science* **2014**, *344*, 616−619.
(16) Choi, M.; Wu, Z. J.; Iglesia, E. *J. Am. Chem. Soc.* **2010**, *132*, 9129−9137.
(17) Schroeder, F.; Esken, D.; Cokoja, M.; van den Berg, M. W. E.; Lebedev, O. I.; van Tendeloo, G.; Walaszek, B.; Buntkowsky, G.; Limbach, H. H.; Chaudret, B.; Fischer, R. A. *J. Am. Chem. Soc.* **2008**, *130*, 6119−6130.
(18) Pan, X. L.; Fan, Z. L.; Chen, W.; Ding, Y. J.; Luo, H. Y.; Bao, X. H. *Nat. Mater.* **2007**, *6*, 507−511.
(19) Chamberlain, T. W.; Zoberbier, T.; Biskupek, J.; Botos, A.; Kaiser, U.; Khlobystov, A. N. *Chem. Sci.* **2012**, *3*, 1919−1924.
(20) Zoberbier, T.; Chamberlain, T. W.; Biskupek, J.; Kuganathan, N.; Eyhusen, S.; Bichoutskaia, E.; Kaiser, U.; Khlobystov, A. N. *J. Am. Chem. Soc.* **2012**, *134*, 3073−3079.
(21) Pan, X. L.; Bao, X. H. *Acc. Chem. Res.* **2011**, *44*, 553−562.
(22) Khlobystov, A. N. *ACS Nano* **2011**, *5*, 9306−9312.
(23) Chen, W.; Fan, Z. L.; Pan, X. L.; Bao, X. H. *J. Am. Chem. Soc.* **2008**, *130*, 9414−9419.
(24) Chen, Z. J.; Guan, Z. H.; Li, M. R.; Yang, Q. H.; Li, C. *Angew. Chem., Int. Ed.* **2011**, *50*, 4913−4917.
(25) Chamberlain, T. W.; Earley, J. H.; Anderson, D. P.; Khlobystov, A. N.; Bourne, R. A. *Chem. Commun.* **2014**, *50*, 5200−5202.
(26) Chen, W.; Pan, X. L.; Bao, X. H. *J. Am. Chem. Soc.* **2007**, *129*, 7421−7426.
(27) Zhang, F.; Pan, X. L.; Hu, Y. F.; Yu, L.; Chen, X. Q.; Jiang, P.; Zhang, H. B.; Deng, S. B.; Zhang, J.; Bolin, T. B.; Zhang, S.; Huang, Y. Y.; Bao, X. H. *Proc. Natl. Acad. Sci. U.S.A.* **2013**, *110*, 14861−14866.
(28) Yan, F. W.; Zhang, S. F.; Guo, C. Y.; Li, F. B.; Yan, F.; Yuan, G. Q. *Catal. Commun.* **2009**, *10*, 1689−1692.
(29) Saqer, S. M.; Kondarides, D. I.; Verykios, X. E. *Top. Catal.* **2009**, *52*, 517−527.
(30) Kim, K. J.; Ahn, H. G. *Appl. Catal., B* **2009**, *91*, 308−318.
(31) Bendahou, K.; Cherif, L.; Siffert, S.; Tidahy, H. L.; Benaissa, H.; Aboukais, A. *Appl. Catal., A* **2008**, *351*, 82−87.
(32) Radic, N.; Grbic, B.; Terlecki-Baricevic, A. *Appl. Catal., B* **2004**, *50*, 153−159.
(33) Briot, P.; Auroux, A.; Jones, D.; Primet, M. *Appl. Catal.* **1990**, *59*, 141−152.
(34) Gland, J. L.; Sexton, B. A.; Fisher, G. B. *Surf. Sci.* **1980**, *95*, 587−602.
(35) Gland, J. L.; Korchak, V. N. *Surf. Sci.* **1978**, *75*, 733−750.
(36) Borgna, A.; Normand, F.; Garetto, T.; Apesteguia, C. R.; Moraweck, B. *Catal. Lett.* **1992**, *13*, 175−188.
(37) Mostafa, S.; Behafarid, F.; Croy, J. R.; Ono, L. K.; Li, L.; Yang, J. C.; Frenkel, A. I.; Cuenya, B. R. *J. Am. Chem. Soc.* **2010**, *132*, 15714−15719.
(38) Manyar, H. G.; Morgan, R.; Morgan, K.; Yang, B.; Hu, P.; Szlachetko, J.; Sa, J.; Hardacre, C. *Catal. Sci. Technol.* **2013**, *3*, 1497−1500.
(39) Zhang, P.; Sham, T. K. *Phys. Rev. Lett.* **2003**, *90*, 245502.
(40) Friebel, D.; Viswanathan, V.; Miller, D. J.; Anniyev, T.; Ogasawara, H.; Larsen, A. H.; O'Grady, C. P.; Norskov, J. K.; Nilsson, A. *J. Am. Chem. Soc.* **2012**, *134*, 9664−9671.
(41) Dege, P.; Pinard, L.; Magnoux, P.; Guisnet, M. *C. R. Acad. Sci., Ser. IIc: Chim* **2001**, *4*, 41−47.
(42) Tsou, J.; Pinard, L.; Magnoux, P.; Figueiredo, J. L.; Guisnet, M. *Appl. Catal., B* **2003**, *46*, 371−379.

DOI: 10.1021/cs501763k
ACS Catal. 2015, 5, 1381−1385